SUPPORTING INFORMATION

The electric field distributions of Au nanorods with semispherical ends (each nanorod corresponding to the size of three coupled spherical Au nanoparticles) are simulated using FDTD, which are shown here for one, two and four nanorods in Figure S1. The similarity of the electric field maps of these Au nanorods and coupled Au nanoparticles support our observation that plasmon coupled Au nanoparticles assembled on top of each other forms nanorod-like structures. These numerical simulations also reveal that these nanorods lead to a stronger electron field localization creating plasmon resonators between them. As the number of nanorods is increased, there are more of these plasmon resonators between every adjacent two of them.

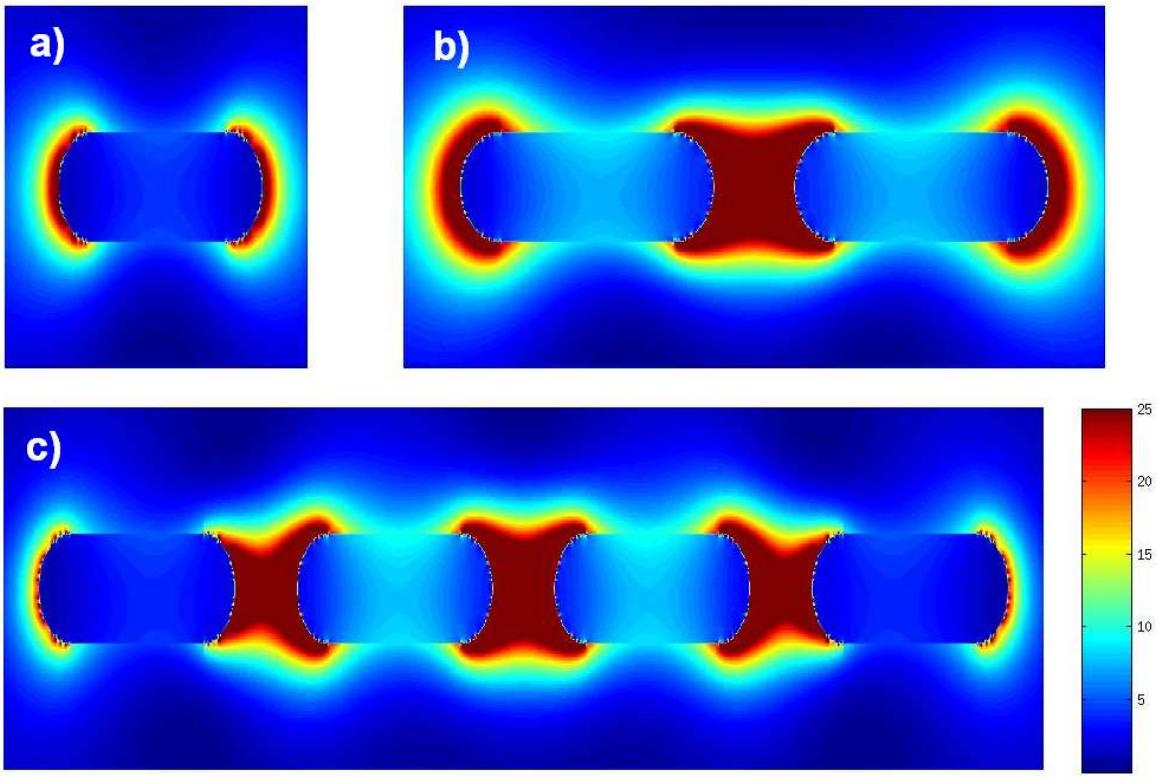

Figure S1. Electric field distribution of (a) one, (b) two, and (c) four Au nanorods with half sphere ends.

The absorption spectrum of our Au nanocolloids is obtained with a peak maximum at 520 nm with a full width half maximum of around 80-90 nm as depicted in Figure S2.

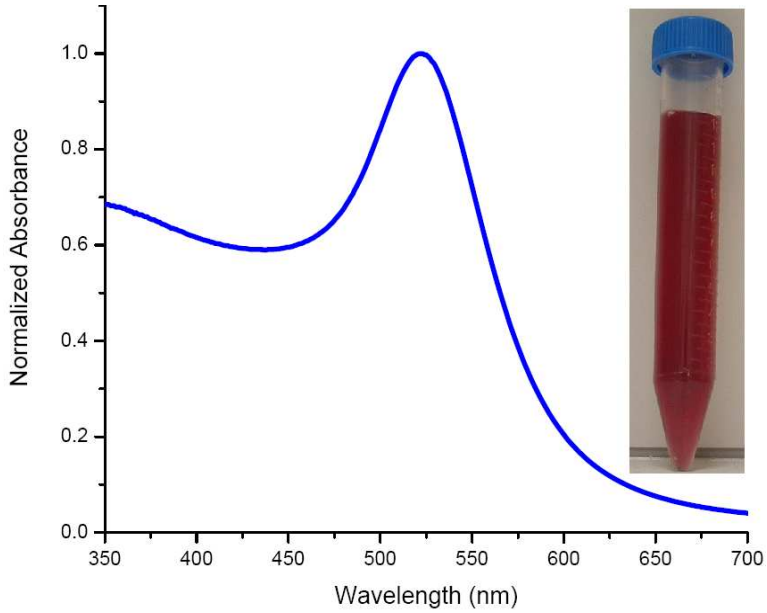

Figure S2. Optical absorption spectrum of our colloidal Au nanoparticles. Inset is a picture of our Au nanoparticles in vial after synthesis.

This synthesis results in an average particle size of 15 nm with an expected size dispersion of 10% as shown in transmission electron microscopy image depicted in Figure S3.

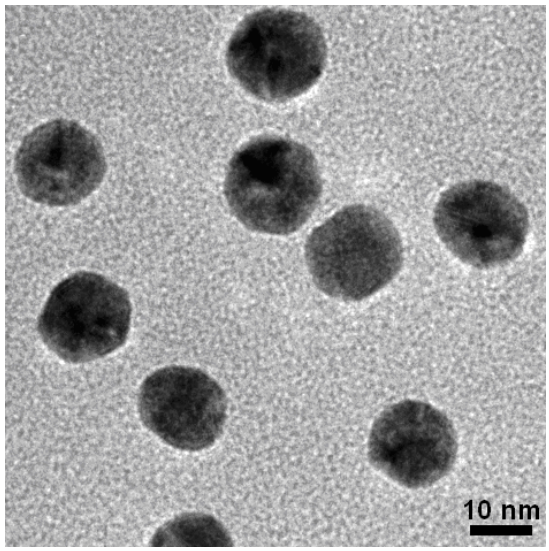

Figure S3. Transmission electron microscopy image of Au nanoparticles.

Synthesis of green NCs are completed after the first couple of minutes and the peak emission wavelength of nanocrystal can further be tuned to longer wavelengths by increasing the synthesis duration if desired as shown in Figure S4.

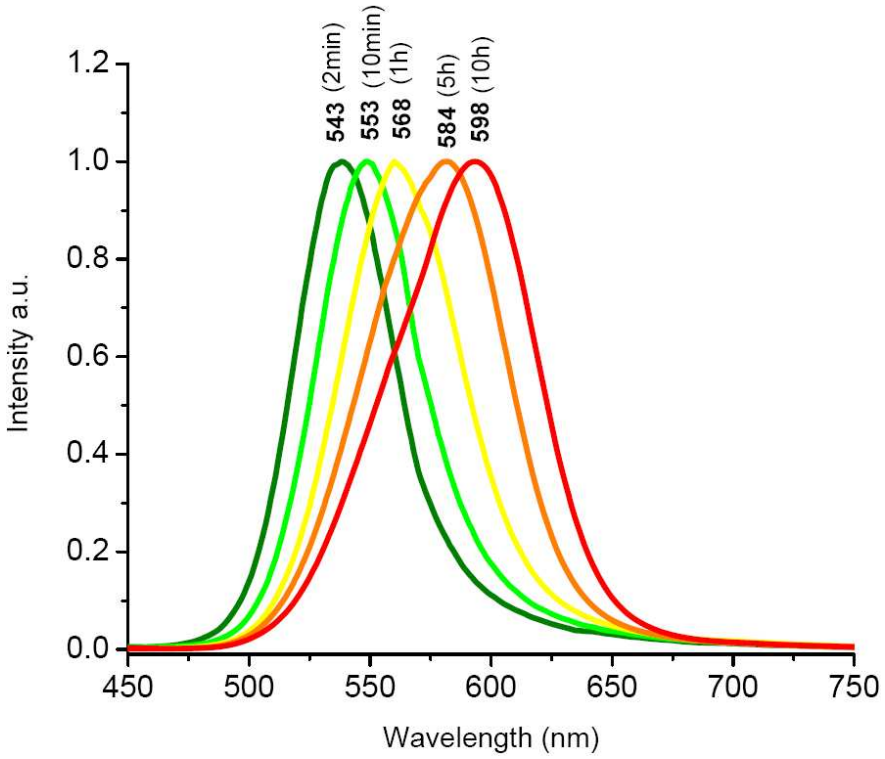

Figure S4. Normalized photoluminescence spectra of our CdTe NCs emitting at successively longer wavelengths which correspond to increased synthesis durations.

A picture of our synthesized CdTe NCs under UV light illumination is depicted in Figure S5.

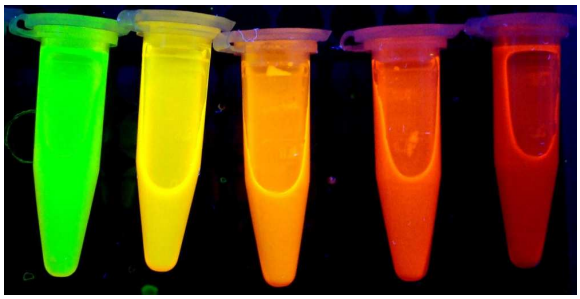

Figure S5. A picture of our CdTe nanocrystals synthesized to emit in different colors, tuned from left to right by increasing the synthesis duration.

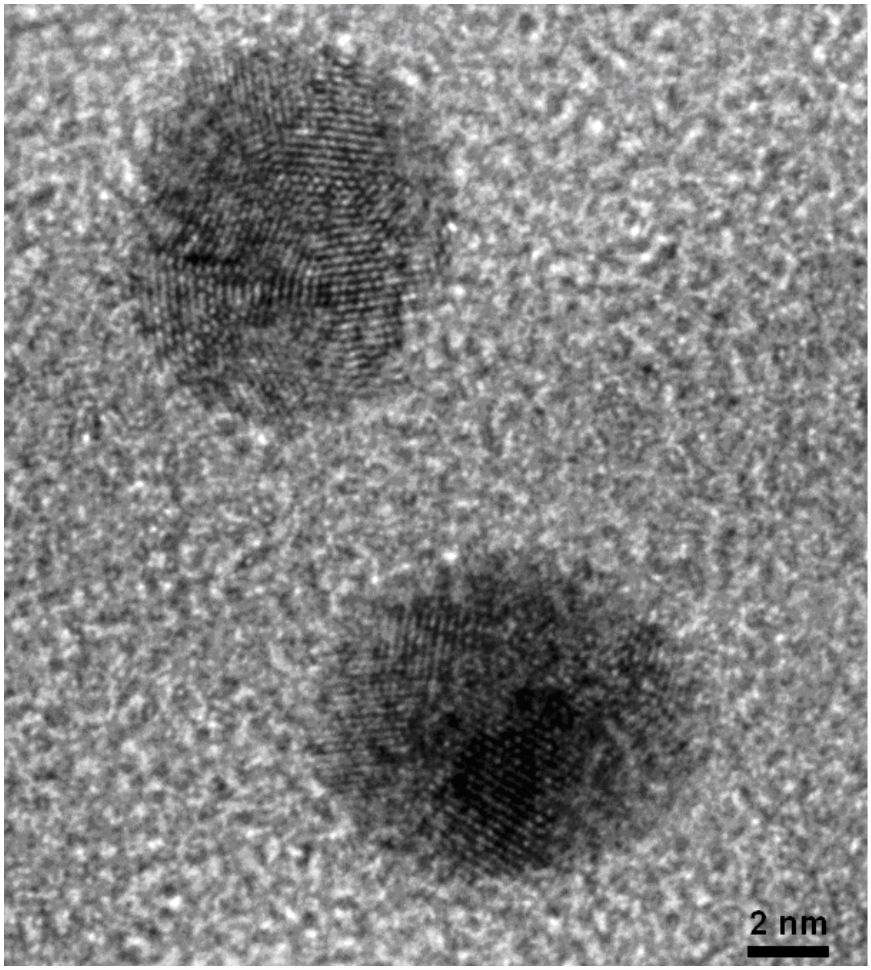

Figure S6. High resolution transmission electron microscopy (HRTEM) image of CdTe nanocrystals. The scale bar is 2 nm.

Atomic force microscope topography of one Au NP monolayer coated corning glass substrate shows that surface coverage is low and Au nanoparticles are easily detected from the surface profile of the red line as depicted in Figure S7.

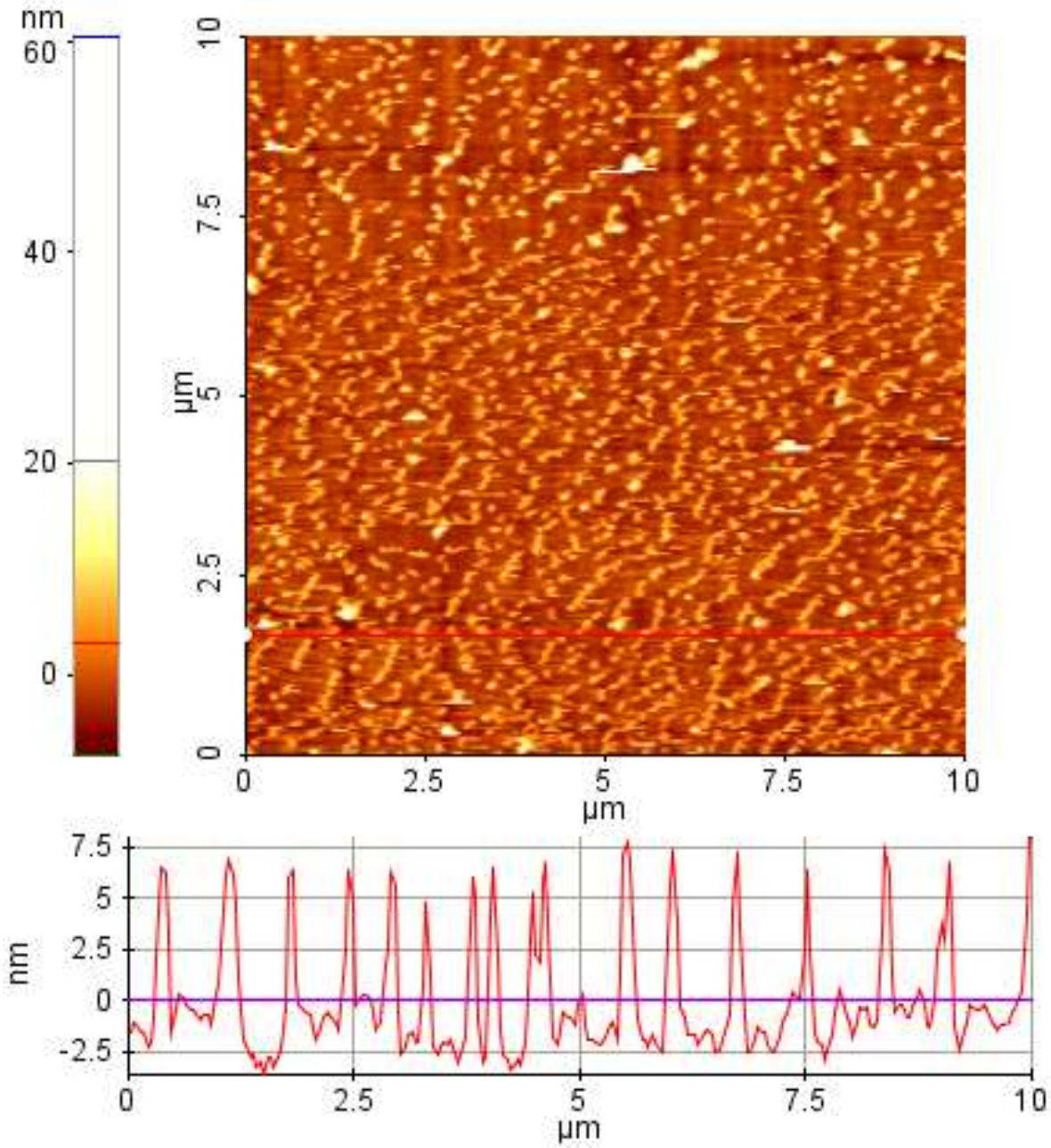

Figure S7. Atomic force microscopy image and surface profile of one monolayer Au nanoparticles coated sample (depicted across the red line).

Atomic force microscope topography of 3 Au NP monolayer coated corning glass substrate shows that surface coverage is 100% and the surface roughness is low except for some small localized regions where more Au nanoparticles have accumulated, as depicted in Figure S8, along with a surface profile across the red line.

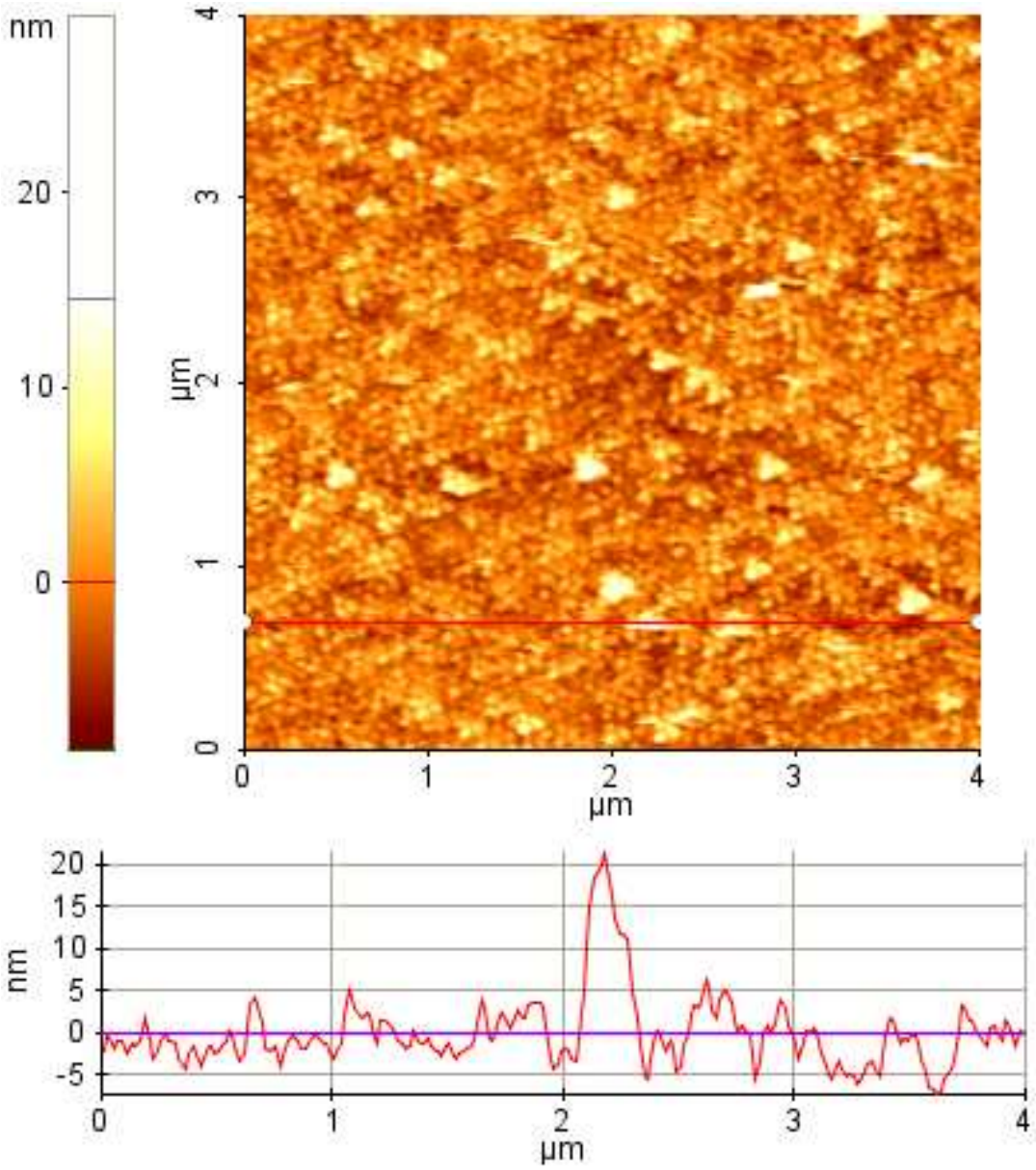

Figure S8. Atomic force microscopy image and surface profile of a three-monolayer Au nanoparticles coated sample (depicted across the red line).

For the decay lifetime analysis, we used the exponential model (reconvolution) and fit the decay curve by the use of commercially available FluoFit software package that comes with the time-resolved setup from Picoquant GmbH. This software program uses the function in equation S1 to fit the decay curve by the use of a high performance computer.

$$I(t) = \int_{-\infty}^{t} IRF(t') \sum_{i}^{n} A_i e^{-\frac{t-t'}{\tau_i}} dt' \tag{S1}$$

In this function for an n-exponential decay fit parameters A_i and τ_i stand for the amplitude and the decay lifetime of the i^{th} component, respectively. IRF is the abbreviation of instrument response function, which is deconvolved from the measured decay curve to eliminate excitation source-detector response related errors in decay analysis of the sample. In our analysis, we start from the single exponential case and check for the decay fit quality factor X^2. For a good match between the experimentally measured decay curve and the calculated decay curve to obtain an X^2 value close to unity, we used a double or a triple exponential fit for the quantum dot solids, and triple exponential fit for the plasmon coupled quantum dot solids.

For anisotropy measurements we used the setup illustrated in Figure S9. A picosecond laser source with an excitation wavelength of 375 nm aligned in vertical polarization is used to excite the substrate. Laser beam is passed through a high precision vertical polarizer and focused on the substrate using high quality lens systems. Also the emitted light is passed through a UV filter (400 nm cut-off wavelength) to eliminate collection of excitation source reflections from the substrate. Filtered light is passed through a linear polarizer in vertical and horizontal polarizations to find the corresponding I_{VV} and I_{VH} emission intensity components. Light is passed through a monochromator with 0.5 mm slits and the photons are counted via a high precision time-correlated single photon counting system (Picoquant-FluoTime200). Data

is analyzed with the assist of a computer using the commercially available software FluoFit by PicoQuant GmbH, Germany.

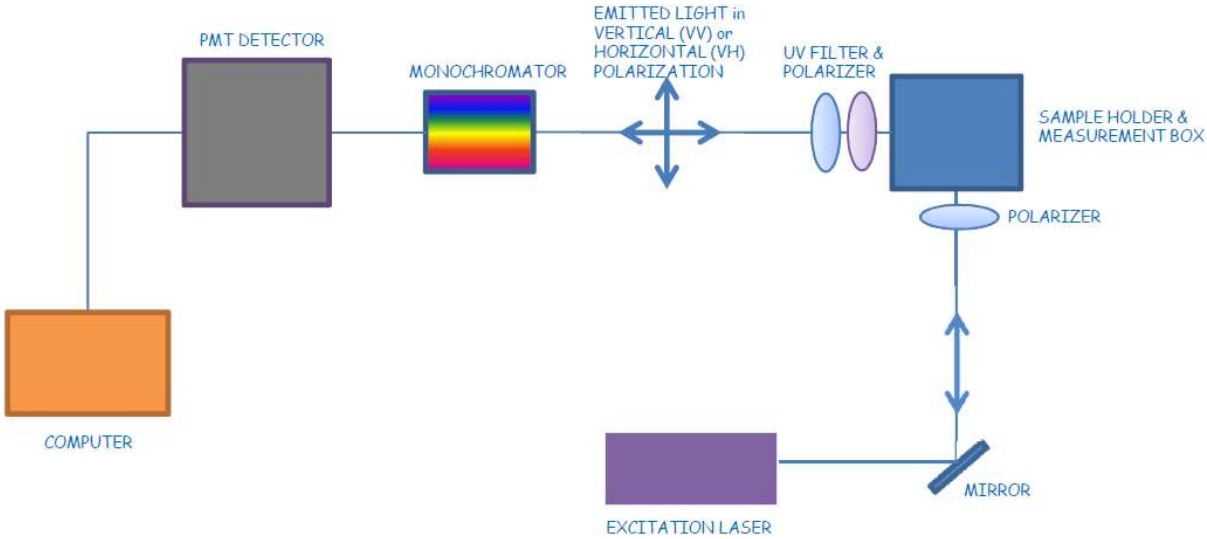

Figure S9. Illustration of our optical setup for anisotropy measurements.

In optical setups such as monochoromators and photo multiplier tubes can be sensitive to the polarization of the light. Such polarization dependency of instruments may lead to substantial errors in fluorescence anisotropy measurements. Calculation of correction factor (G-factor) is a powerful method to minimize instrumental errors. To calculate the G-factor we used the setup illustrated in Figure S10. Using the ratio of collected emission intensities in different polarizations as given in equation (1) of our manuscript gives the G-factor value.

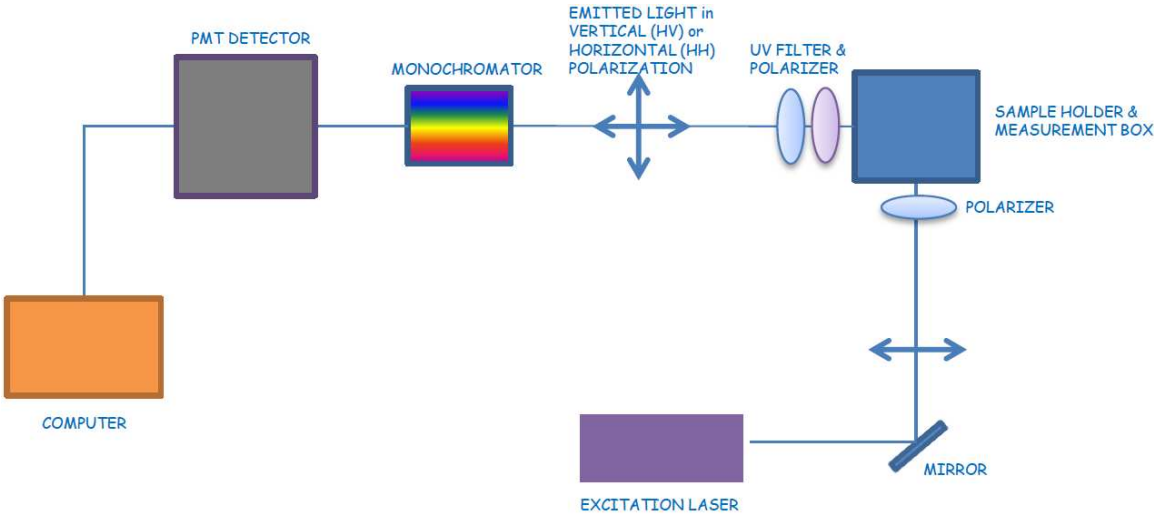

Figure S10. Illustration of our optical setup for G-factor measurement.